Volume reconstruction based on non-rigid registration

Xudong Bao [1 2 *], **Danhua Xu** [1 2], **Christine Toumoulin** [1 3 *], **Limin M. Luo** [1 2 *]

[1] *CRIBS, Centre de Recherche en Information Biomédicale sino-français INSERM : Laboratoire International Associé , Université de Rennes 1 , SouthEast University , Rennes, FR*

[2] *LIST, Laboratory of Image Science and Technology* [*Nanjing*] *SouthEast University , School of Computer Science and Engineering , Si Pai Lou 2, Nanjing, 210096, CN*

[3] *LTSI, Laboratoire Traitement du Signal et de l'Image INSERM : U642 , Université de Rennes 1 , Campus de Beaulieu, 263 Avenue du Général Leclerc - CS 74205 - 35042 Rennes Cedex, FR*

* Correspondence should be addressed to: Xudong Bao <bao.list@seu.edu.cn >
* Correspondence should be addressed to: Christine Toumoulin <christine.toumoulin@univ-rennes1.fr >
* Correspondence should be addressed to: Limin Luo <luo.list@seu.edu.cn >

Abstract

Volume reconstruction is one of the key problems in 3D image rendering and analysis. Inter slice interpolation methods have been widely discussed in the literature and object-based algorithms have been shown to well behave. In this paper, we present a non-rigid registration based strategy to improve the volume reconstruction. A level set evolution technique is proposed to yield the deformation between adjacent slices. A modified bilinear interpolation method is then designed to generate propagating image. A multi-resolution scheme is applied to decrease the computation time and support large deformation. The resulting images show good results on regions enclosing different anatomic structures.

MESH Keywords Brain ; Humans ; Image Interpretation, Computer-Assisted ; Magnetic Resonance Imaging

Author Keywords interpolation ; non-rigid registration ; level set

Introduction

Medical imaging devices such as CT or MRI generally produce a set of slices in which the dimension of the voxel is not isotropic, i.e. the distance between two successive slices is larger than the distance between two neighboring pixels within a slice. An interpolation technique is thus required to improve the axial resolution between slices before applying any visualization or analysis technique on the data volume.

Many interpolation techniques have been proposed in the literature [1–7]. They classically fall into two main categories: scene-based and object-based methods. In scene-based methods the interpolation is only based on the image intensities. Let's cite for instance, the nearest neighbor method, the linear one or the spline-based interpolation functions. Comparisons of these methods have been published by Meijering [2] and Thevenaz [3]. They suppose that the pixels used in the original slices, to compute the pixels in the missing slice, belong to the same anatomic structure. This is rarely the case. When the structure shifts considerably from one slice to another (due to a deformation of the structure), the interpolation method produces artifacts on the new created slice. Object-based interpolation methods rely on additional information previously extracted from the slices to guide the interpolation process. The interpolation is then only performed between pixels belonging to the same anatomic structures on the different slices. Some of these methods performed a preliminary shape matching between the slices prior to interpolation [4–6]. This stage involves performing a preliminary segmentation of the structures all over the slices. This task remains difficult and computationally expensive. Other methods involve a preliminary intensity based registration between adjacent slices before interpolating between corresponding positions in each slice[7–8]. These techniques used the optical flow or mixed intensity and gradient information to match pixels between slices. A lot of non linear registration techniques have been described in the literature [7].

Level set techniques have been widely discussed to depict curve or surface deformation [8–9]. The level sets evolve from initial position based on spatio-temporal partial differential equations (PDEs) in distance space. Vemuri, et al. presented a level set based non-rigid registration method [10].

Our volume reconstruction method is based on the object-based scheme and the level set is used to estimate the deformation between slices. A modified bilinear interpolation method is designed for the propagation of gray image. A multi-resolution scheme is applied to optimize the computation and trace the large size deformation. Results are given on brain MRI slices.

Methods

Level Set Based Non-rigid Registration Scheme

Osher and Senthian [11] presented elementary spatio-temporal PDE

$$\frac{\partial \Phi}{\partial t} + \mathbf{v} \cdot \nabla \Phi = 0,$$

(1)

which converts the level set values (levels) with the velocity field **v** , where Φ is level set function (distance function). If only the motion on normal direction is taken into account, (1) becomes

$$\frac{\partial \Phi}{\partial t} + v_N |\nabla \Phi| = 0,$$

(2)

where $v_N = \mathbf{v} \cdot \frac{\nabla \Phi}{|\nabla \Phi|}$.

Usually, the contours on image plane are mapped to zero level sets in distance space. Because the level sets evolve in higher dimensional space than image plane, the topological change of contours can be easily performed during evolution.

Vemuri *et al*. defined the distance function Φ to be image gray levels and introduced level set based non-rigid registration method [10]. The registration of two images is given by the evolution of the gray levels of the intensity function from source image I_1 to that of target image I_2 . The velocity of evolution on normal direction is selected as the gray level difference between two images. Then, (2) can be rewritten as [10],

$$I_t(\mathbf{X}, t) = (I_2(\mathbf{X}) - I(\mathbf{X}, t))|\nabla I(\mathbf{X}, t)|,$$

(3)

with $I(\mathbf{X},0)=I_1(\mathbf{X})$, where $\mathbf{X}=(x, y)^T$ is the position of pixel, $I_t(\mathbf{X},t)$ denotes the increment of image intensities at time t.

Suppose that adjacent slices contain similar anatomic structures and same anatomic structures have similar gray levels. Fortunately, the assumption is satisfied for adjacent slices from most tomographic imaging devices. Based on the assumption, the gray level evolution can be equivalently considered as the deformation of source image. A similar approach was presented [10],

$$\mathbf{V}_t = [I_2(\mathbf{X}) - I_1(\mathbf{V}(\mathbf{X}))] \frac{\nabla I_1(\mathbf{V}(\mathbf{X}))}{|\nabla I_1(\mathbf{V}(\mathbf{X}))|},$$

(4)

where $\mathbf{V}=(u, v)^T$ denotes the displacement vector at **X** and the operation $\mathbf{V}(\mathbf{X})=(x-u, y-v)^T$ translates position **X** at the opposite direction of **V** . The normalized gradient at the right side of (4) defines normal of evolution. The stable solution of **V** from (4) registers source image I_1 to target image I_2 .

Because the gradient operation is very sensitive to noise, the image is convolved with a Gaussian filter kernel with standard derivation σ before the gradient operation [10],

$$\mathbf{V}_t = [I_2(\mathbf{X}) - I_1(\mathbf{V}(\mathbf{X}))] \frac{\nabla (G_\sigma * I_1(\mathbf{V}(\mathbf{X})))}{|\nabla (G_\sigma * I_1(\mathbf{V}(\mathbf{X})))| + \alpha}$$

(5)

Positive constant α is selected to stabilize the computation when the denominator is close to zero.

Numerical implementation

Malladi *et al*. presented the numerical implementation of non-linear hyperbolic PDEs in detail [12]. This numerical scheme can be used in the implementation of Eq. (5) except the propagation of the distance image (gray level image). Usually, in numerical implementation of level set equations, the increment of distance function at each position on distance image is computed and then the distance function is simply updated during each iterative step. But, Eq. (5) explicitly defines the modification of deformation matrix of image grids from I_1 to propagated image I_t instead of the increment of distance function. Thus, the distance image will be updated by deforming I_1 based on the deformation matrix. An appropriate interpolation method has to be adopted to compute the gray levels of discrete image depending on the pixels at twisted grids mapped from I_1 .

For each pixel $\mathbf{X}'$ of discrete image I_t , a minimal surrounding quadrangle can be found, which four vertices, denoted as $\mathbf{X}'_1$, $\mathbf{X}'_2$, $\mathbf{X}'_3$ and $\mathbf{X}'_4$, are mapped from corresponding pixels $\mathbf{X}_1$, $\mathbf{X}_2$, $\mathbf{X}_3$, and $\mathbf{X}_4$ on image I_1 by deformation matrix, shown as Fig. 1. Based on the assumption that the gray levels of the pixels will not change during deformation, we have $I_t(\mathbf{X}'_1) = I(\mathbf{X}_1)$, $I_t(\mathbf{X}'_2) = I(\mathbf{X}_2)$, $I_t(\mathbf{X}'_3) = I(\mathbf{X}_3)$ and $I_t(\mathbf{X}'_4) = I(\mathbf{X}_4)$, although the position $\mathbf{X}'_1$, $\mathbf{X}'_2$, $\mathbf{X}'_3$ and $\mathbf{X}'_4$ may be not discrete coordinates. The modified bilinear interpolation method is designed to estimate the pixel gray level based on pixels at the vertices of surrounding quadrangle other than rectangle. The

scheme is divided into two steps. Firstly, a linear interpolation is applied to left vertices pair ($\mathbf{X}'_1$ and $\mathbf{X}'_4$) and right vertices pair ($\mathbf{X}'_2$ and $\mathbf{X}'_3$) respectively. Suppose that $\mathbf{X}'_L$ is the dot on line $\mathbf{X}'_1\mathbf{X}'_4$ closest to $\mathbf{X}'$ (in the figure, $\mathbf{X}'_L$ has the same position with $\mathbf{X}'_1$), and $\mathbf{X}'_R$ is the dot on line $\mathbf{X}'_2\mathbf{X}'_3$ closest to X′. The gray levels at $\mathbf{X}'_L$ and $\mathbf{X}'_R$ are respectively interpolated by

$$I_t^L(\mathbf{X}') = \frac{|\overrightarrow{\mathbf{X}'_1\mathbf{X}'}|}{|\overrightarrow{\mathbf{X}'_1\mathbf{X}'}|+|\overrightarrow{\mathbf{X}'_4\mathbf{X}'}|} I_1(\mathbf{X}_4) + \frac{|\overrightarrow{\mathbf{X}'_4\mathbf{X}'}|}{|\overrightarrow{\mathbf{X}'_1\mathbf{X}'}|+|\overrightarrow{\mathbf{X}'_4\mathbf{X}'}|} I_1(\mathbf{X}_1)$$

(6)

and

$$I_t^R(\mathbf{X}') = \frac{|\overrightarrow{\mathbf{X}'_2\mathbf{X}'}|}{|\overrightarrow{\mathbf{X}'_2\mathbf{X}'}|+|\overrightarrow{\mathbf{X}'_3\mathbf{X}'}|} I_1(\mathbf{X}_3) + \frac{|\overrightarrow{\mathbf{X}'_3\mathbf{X}'}|}{|\overrightarrow{\mathbf{X}'_2\mathbf{X}'}|+|\overrightarrow{\mathbf{X}'_3\mathbf{X}'}|} I_1(\mathbf{X}_2).$$

(7)

Then, the gray level of pixel $\mathbf{X}'$ is interpolated from $I_t^L(\mathbf{X}')$ and $I_t^R(\mathbf{X}')$ by

$$I_t(\mathbf{X}') = \frac{|\overrightarrow{\mathbf{X}'_L\mathbf{X}'}|}{|\overrightarrow{\mathbf{X}'_L\mathbf{X}'}|+|\overrightarrow{\mathbf{X}'_R\mathbf{X}'}|} I_t^R(\mathbf{X}') + \frac{|\overrightarrow{\mathbf{X}'_R\mathbf{X}'}|}{|\overrightarrow{\mathbf{X}'_L\mathbf{X}'}|+|\overrightarrow{\mathbf{X}'_R\mathbf{X}'}|} I_t^L(\mathbf{X}').$$

(8)

In numerical implementation the displacement of deformation matrix, $\Delta\mathbf{V}(\mathbf{X}, t)$, is computed by applying the numerical scheme presented by [12] to Eq. (5) during each iterative step. The deformation matrix $\mathbf{V}$ is updated by normalized $\Delta\mathbf{V}(\mathbf{X}, t)$ for the stability, i.e.

$$\mathbf{V}(\mathbf{X}, t+1) = \mathbf{V}(\mathbf{X}, t) + \frac{\Delta\mathbf{V}(\mathbf{X}, t)}{\max_{\mathbf{X}}\{|\Delta\mathbf{V}(\mathbf{X}, t)|\}}.$$

(9)

Each pixel on original image I_1 is mapped to propagated image plane by deformation matrix $\mathbf{V}$. Then, the discrete propagated image I_t is interpolated with presented modified bilinear interpolation method. The iteration will be stopped if the maximum of $\Delta\mathbf{V}$ is less than a threshold.

A multi-resolution strategy is adopted to reduce computation time and improve the stability of the propagation by applying a coarse-to-fine registration process.

Volume Reconstruction

The registration depicts the geometric transformation $\mathbf{V}$ between slices. The each element of $\mathbf{V}$ maps one pixel on slice I_1 to corresponding position on slice I_2, which is benefited from level set based registration scheme. The linear interpolation of gray levels is taken place between the corresponding pixels on two adjacent slices, which will reduce the artifacts in the boundary area of anatomic structures.

Suppose that the distance between two slices is *z*, and the interpolated image is *d* from slice 1. The deformation from slice 1 to interpolating plane, denoted as $\mathbf{V}_d$, will be *d*/*z* times $\mathbf{V}$, shown as Fig. 2. Let $\mathbf{X}_d$ be the cross point where line $\mathbf{X}\mathbf{X}'$ passes through interpolation plane I_d. The gray level at $\mathbf{X}_d$, denoted $I_d(\mathbf{X}_d)$, can be decided by linear interpolation between corresponding pixels $\mathbf{X}$ and $\mathbf{X}'$,

$$I_d(\mathbf{X}_d) = \frac{d}{z} I_2(\mathbf{V}(\mathbf{X})) + (1 - \frac{d}{z}) I_1(\mathbf{X}).$$

(10)

Each element of deformation matrix $\mathbf{V}$ defines a pair of corresponding pixels respectively on I_1 and I_2, and, then, a pixel, which may locate within coordinate grid, can be evaluated. Based on the pixels, the discrete image on interpolation plane can be obtained by applying presented modified bilinear interpolation method again.

Results

In the experiment, three consecutive slices were selected from MRI sequence with 2mm intervals to test the performance of the methods, shown in Fig. 3 (a)–(c). The size of images was 256×256 and the dimension of each pixel was 0.9375mm × 0.9375mm. The middle slice, shown in Fig. 3(b), was removed from the sequence and the image at the position of the middle slice was interpolated based on first and last slices. The difference between the interpolated image and the removed middle slice was analyzed for the evaluation of the

methods. All computations were done on PC with P4 2.66GHz CPU and 512M memory, and the program was encoded with Microsoft Visual C++.

The level set based methods were applied to the interpolation. The multi-resolutional registration was applied in three different resolution stages, i.e. 32×32, 128×128 and 256×256 resolution levels. The coarse images were resampled from original slices by averaging pixels within correlative region. We set the standard derivation σ of Gaussian filter in Eq. (5) to 1.0 and α to 0.01. The final deformation registered between the first and last images was shown in Fig. 3(e). The linear interpolation was applied between corresponding pixels defined by the deformation matrix and the modified bilinear interpolation method was chosen to get discrete image, shown as Fig. 3(d). All the process took less than 2s. An image of the absolute differences between the interpolated image and the original slice was shown in Fig. 3(f). The mean square root of the difference image was 11.6.

For the comparison, we applied traditional linear interpolation method and [7] presented methods to the experiment data respectively. The results were shown in Fig. 3(g) and Fig. 3(i) and the images of absolute differences between interpolated images and the original slice were given by Fig. 3(h) and Fig. 3(j), where the differences were normalized to [0,255]. The mean square root of the difference images were 20.9 and 16.2 respectively.

Conclusion

We have applied level set based non-rigid registration to volume reconstruction and designed a modified bilinear interpolation scheme applied to the propagation of gray level image in registration process and the estimation of interpolated image. The results indicated that the anatomic structures were well kept on interpolated image.

References:

- 1 . Grevera GJ , Udupa JK . An objective comparison of 3-D image interpolation methods . IEEE Trans Med Imag . 17 : (8) 1998 ; 642 - 652
- 2 . Meijering EHW , Niessen WJ , Viergever MA . Quantitative evaluation of convolution-based methods for medical image interpolation . Med Image Anal . 5 : (2) 2001 ; 111 - 126
- 3 . Thevenaz P , Blu T , Unser M . Interpolation revisited . IEEE Trans Med Imag . 19 : (7) 2000 ; 739 - 758
- 4 . Herman GT , Zheng J , Bucholtz CA . Shape-based interpolation . IEEE Comput Graph Appl . 12 : 1992 ; 69 - 79
- 5 . Raya SP , Udupa JK . Shape-based interpolation of multidimensional objects . IEEE Trans Med Imag . 9 : (5) 1990 ; 32 - 42
- 6 . Higgins WE , Morice C , Ritman EL . Shape-based interpolation of tree-like structures in three-dimensional images . IEEE Trans Med Imag . 12 : (9) 1993 ; 439 - 450
- 7 . Penny GP , Schnable JA , Rueckert D , Viergever MA , Niessen WJ . Registration-based interpolation . IEEE Trans Med Imag . 23 : (7) 2004 ; 922 - 926
- 8 . Osher S , Fedkiw RP . Level set methods: an overview and some recent results . J Comput Phys . 169 : 2001 ; 463 - 502
- 9 . Liao G , Liu F , Pena GC , Peng D , Osher S . Level-set-based deformation methods for adaptive grids . J Comput Phys . 159 : 2000 ; 103 - 122
- 10 . Vemuri BC , Ye J , Chen Y , Leonard CM . Image registration via level-set motion: Applications to atlas-based segmentation . Med Imag Anal . 7 : 2003 ; 1 - 20
- 11 . Osher S , Senthian JA . Fronts propagating with curvature dependent speed: algorithms based on Hamilton-Jacobi formulations . J Comput Phys . 79 : 1988 ; 12 - 49
- 12 . Malladi R , Sethian JA , Vemuri BC . Shape modeling with front propagation: A level set approach . IEEE Trans PAMI . 17 : (2) 1995 ; 158 - 175

Fig. 1

Pixel **X** ′ and its minimal surrounding quadrangle

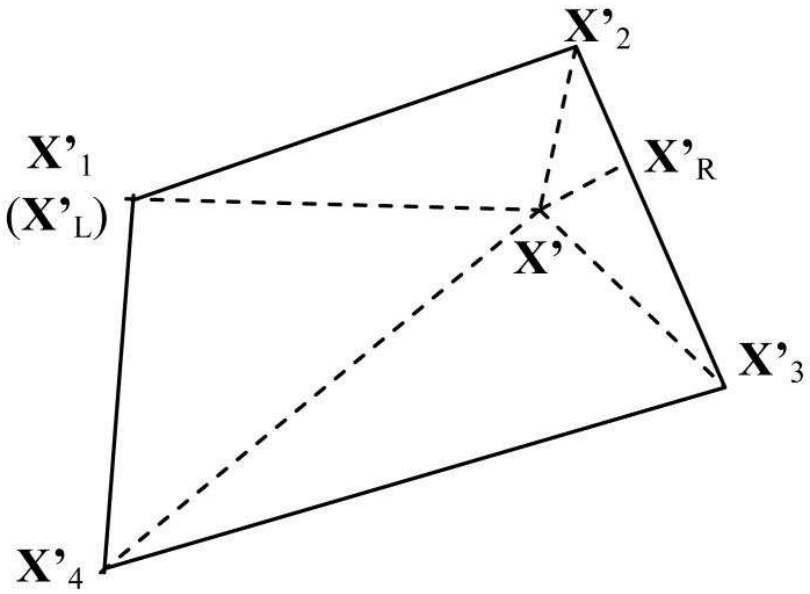

Fig. 2

The registered positions of pixels on slices and interpolation plane

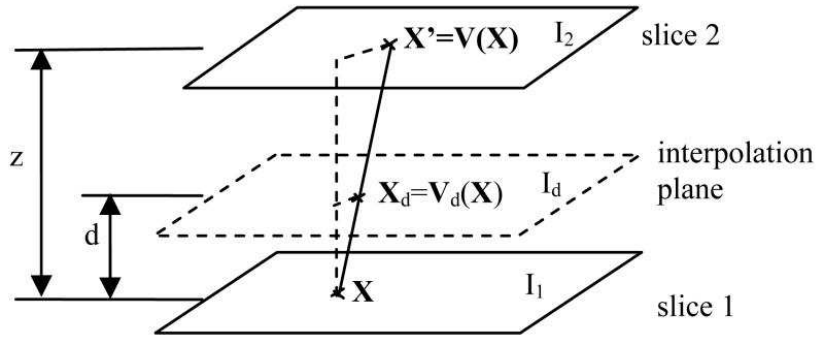

Fig. 3

(a) – (c) three consecutive slices from MRI slice sequence with 2mm intervals, (d) the interpolated image between slice (a) and (c) at the position of slice (b) based on the presented method, (e) the displacement field depicting the deformation between (a) and (c), (f) absolute differences between (d) and (b), (g) the interpolated image with linear interpolation, (h) the absolute differences between (g) and (b), (i) image based on method described in [7], (j) the absolute differences between (i) and (b)